NATIONAL ADVISORY COMMITTEE FOR AERONAUTICS

WARTIME REPORT

ORIGINALLY ISSUED

July 1946 as Memorandum Report L6F27

AERODYNAMIC CHARACTERISTICS OF SEVERAL MODIFICATIONS

OF A 0.45-SCALE MODEL OF THE VERTICAL TAIL

OF THE CURITISS XP-62 AIRPLANE

By John G. Lowry, Thomas R. Turner, and Robert B. Liddell

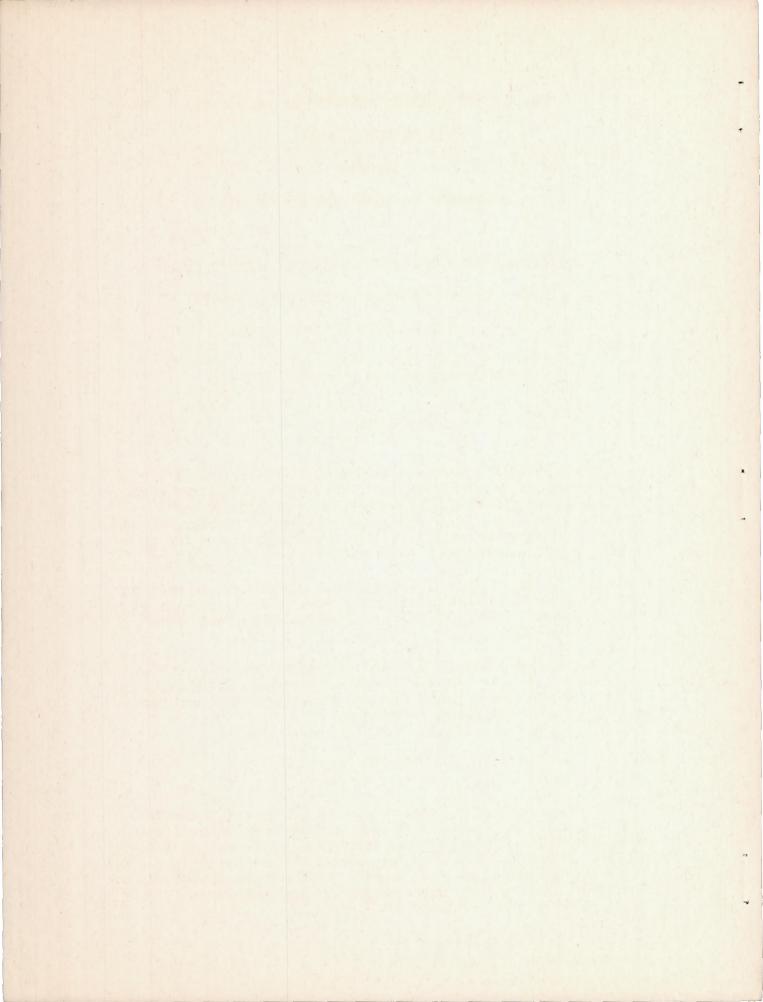
Langley Memorial Aeronautical Laboratory
Langley Field, Va.

CALIFORNIA INSTITUTE OF TECHNOLOGY



WASHINGTON

NACA WARTIME REPORTS are reprints of papers originally issued to provide rapid distribution of advance research results to an authorized group requiring them for the war effort. They were previously held under a security status but are now unclassified. Some of these reports were not technically edited. All have been reproduced without change in order to expedite general distribution.



NACA LANGLEY MEMORIAL AERONAUTICAL LABORATORY

MEMORANDUM REPORT

for the

Air Materiel Command, Army Air Forces

MR No. L6F27

AERODYNAMIC CHARACTERISTICS OF SEVERAL MODIFICATIONS

OF A 0.45-SCALE MODEL OF THE VERTICAL TAIL

OF THE CURTISS XP-62 AIRPLANE

By John G. Lowry, Thomas R. Turner, and Robert B. Liddell

SUMMARY

The 0.45-scale model of the Curtiss XP-62 vertical tail surface mounted on a stub fuselage, was tested in the Langley 7-by 10-foot tunnel. The aerodynamic characteristics of the vertical tail with a plain rudder, two amounts of overhang and an internal balance are presented. Tab characteristics on the plain rudder are also presented.

The results of this investigation indicate that the overhang and the internal balance of about the same balance area have very similar characteristics throughout the angle-of-yaw and rudder-deflection range.

The results indicate that the tab is effective at least to tab angles of ±20° over both the rudder and angle-of-attack range except for the case of large positive angles of attack combined with large negative rudder deflections.

INTRODUCTION

In the course of an investigation to find a satisfactory vertical tail for the XP-62 airplane, a 0.45-scale vertical tail model mounted on a stub fuselage was tested in the Langley 7-by 10-foot tunnel. This model was fitted with a flat plate to represent the horizontal tail surface. The data are presented herein for their general interest value rather than their application to this particular airplane.

The balance arrangements tested consisted of a plain rudder, a medium overhang, a large overhang, and an internal balance.

The results of the model tests are presented herein.

APPARATUS, METHODS, AND TESTS

The test setup in the Langley 7- by 10-foot tunnel is shown in the photograph of figure 1. The model was fastened to a large tube that extended through the floor of the test section and was attached to the balance frame. A streamline fairing that extended almost to the stub fuselage was placed around this tube and fastened to the floor (fig. 1). Provisions were made for changing the angle of attack (yaw) of the model while the tunnel was in operation. The rudder was controlled from outside the tunnel and the rudder and tab hinge moments were measured with electrical strain gages mounted within the rudder.

The model of the vertical tail conformed to the dimensions of figures 2 and 3. The geometric characteristics are given in table I. A 3/4-inch-thick flat plate was provided to represent a horizontal tail surface (fig. 4.)

The several balance arrangements tested are given in the following table:

Designationt	Description	c _b	b _b	S _b S _r	Figure
V14R14	Plain rudder	0.144	1.0	0.142	2
v16 _R 16	Medium overhang	.298	.747	.209	2
V18R18	Large overhang	.494	.747	.349	2
V16R16.5	Internal balance	.284	.747	.198	3

The nose shapes and dimensions of the overhang balances are given in figure 2. The plain rudder and overhang balances were tested both sealed and unsealed. The hinges, however, were not completely sealed. For one series of tests, 0.013-inch-diameter transition wires were placed at the 10-percent-chord point along the vertical surface for the plain rudder V14R14 and around the fuselage just back of the leading-edge radius.

With the internally balanced rudder, two variations in the seal conditions were tested. For one series of tests, the hinges were left unsealed, that is, the flexible seal on the balance plate was in contact with the hinge fittings, but no attempt was made to prevent theair flow around the fittings (fig. 5(a)). In the other series of tests, the hinges were completely sealed with rubber dam that prevented any air leakage (fig. 5(b)).

A dynamic pressure of 16.37 pounds per square foot was maintained for almost all tests. It was reduced slightly for some tests, however, when the rudder deflection and angle of attack were large. A dynamic pressure of 16.37 pounds per square foot corresponds to a tunnel velocity of about 80 miles per hour and to an effective Reynolds number of about 2,464,000 based on the mean geometric chord of 2.06 feet and a wind-tunnel turbulence factor of 1.6 (effective Reynolds number = test Reynolds number × turbulence factor).

COEFFICIENTS AND CORRECTIONS

The results of the tests are presented in standard NACA nondimensional coefficients of forces and moments. The pitching moment is taken about the mounting axis center line shown in figure 2. (13 inches ahead of the rudder hinge axis).

The coefficients and symbols are defined as follows:

C_L lift coefficient (L/qS)

CD drag coefficient (D/qS)

C_m pitching-moment coefficient (M/qSc)

$$c_{h_r}$$
 rudder hinge-moment coefficient $\left(\frac{H_r}{qb_rc_r^2}\right)$

$$C_{h_t}$$
 tab hinge-moment coefficient $\left(\frac{H_t}{q b_f \tilde{c}_f}\right)$

where

L lift, pounds

D drag, pounds

- pitching moment about mounting axis center line, foot-pounds M
- rudder hinge moment about control surface hinge line, foot-Hr pounds
- rudder tab hinge moment about tab hinge line, foot-pounds H+
- tail area, 10.26 square feet S
- Sr rudder area, 4.28 square feet
- balance area Sh
- dynamic pressure (pV2) pounds per square foot
- br rudder span, 4.90 feet
- balance span. 3.47 feet bh
- tab span, 1.31 feet bt.
- tail mean geometric chord, 2.06 feet
- rudder root-mean-square chord, 0.876 feet Cr
- tab root-mean-square chord, 0.299 feet C+
- balance root-mean-square chord Ch

and

- angle of attack or yaw, positive with trailing edge to left a
- rudder deflection, positive with trailing edge to left Sr
- tab deflection, positive with trailing edge to left
- rudder pedal force, pounds

$$c_{L_{\alpha}} = \left(\frac{\partial \alpha}{\partial c_{L}}\right) \delta_{r} = \delta_{t} = 0$$

$$c_{L_{\alpha}} = \left(\frac{\partial c_{L}}{\partial \alpha}\right)_{\delta_{r} = \delta_{t} = 0}$$

$$c_{L_{\delta_{r}}} = \left(\frac{\partial c_{L}}{\partial \delta_{r}}\right)_{\alpha = \delta_{t} = 0}$$

$$c_{L_{\delta_t}} = \left(\frac{\partial c_L}{\partial \delta_t}\right)_{\alpha = \delta_{r} = 0}$$

$$c_{h_{\alpha_{r}}} = \left(\frac{\partial c_{h_{r}}}{\partial \alpha}\right)_{\delta_{r} = \delta_{t} = 0}$$

$$C_{h_{\alpha_t}} = \left(\frac{\partial C_{h_t}}{\partial \alpha}\right)_{\delta_r = \delta_t = 0}$$

$$c_{h_{\delta_r}} = \left(\frac{\partial c_{h_r}}{\partial \delta_r}\right)_{\alpha = \delta_t = 0}$$

$$c_{h_{\delta_t}} = \left(\frac{\partial c_{h_t}}{\partial \delta_t}\right)_{\alpha = \delta_r = 0}$$

The following jet-boundary corrections were applied by addition to the tunnel data:

$$\Delta C_{T} = -0.0176C_{L}$$

$$\Delta C_{\rm D} = 0.0445 C_{\rm L}^2$$

$$\Delta C_{\rm m} = 0.0079C_{\rm L}$$

$$\Delta C_h = (plain rudder) = 0.0123C_L$$

$$\Delta C_h = (50\text{-percent overhang balance}) = 0.089C_L$$

$$\Delta C_h = (30\text{-percent overhang balance and internal balance}) = 0.0110C_I$$

RESULTS AND DISCUSSION

Presentation of data. The results of the tests of the various model configurations are given in figures 6 through 19. Figures 20 through 26 present data that have been replotted or cross plotted in order to show the effects of certain independent variables.

A comparison of the vertical tail and rudder characteristics for small rudder deflections and angles of attack is given in table II.

Lift characteristics. The value of the slope of the lift curve (figs. 6 to 8 and table II) either with or without the horizontal tail in place is somewhat higher than theoretical equations indicate would be the case. It is therefore concluded that the stub fuselage in addition to having considerable end plate effect with the horizontal tail removed, also adds effective area to the vertical tail. This effective area added by the stub fuselage would probably not be present if a complete fuselage were used. Adding the horizontal tail increases this end plate effect on the slope of the lift curve slightly. The effect of the horizontal tail might seem to be very small, but it should be noted (fig. 2) that the horizontal tail is near the center of the effective vertical-tail area of the combination stub fuselage and vertical tail.

The effect of the various overhang balances on the lift characteristics can be seen in the comparison curves of figure 20 and the parameters given in table II. Sealing the balance nose on the plain overhang increased the rudder effectiveness $C_{L\delta_r}$,

the larger effect being found in the medium overhang. The internally balanced rudder showed characteristics similar to those for the plain sealed rudder. Sealing the hinges of the internally balanced rudder increased the rudder effectiveness parameter $c_{L\delta_r}$

by about 10 percent.

Hinge moments. The rudder hinge-moment coefficients were replotted on figures 16 and 17 to a larger scale only to separate the curves and not to imply any greater accuracy.

The reduction in Chor is not directly proportional to the

overhang balance area, the greater reduction in hinge moment occurring between the medium and large overhang than between the plain rudder and medium overhang (fig. 21). This variation in $C_{h\delta r}$ with overhang balance chord is very similar to that which would be estimated from the section data of reference 1.

A comparison of the rudder hinge-moment coefficients for the plain and overhang balanced rudder is presented in figure 21. The internally balanced and sealed rudder vl6Rl6.5, had quite similar characteristics to the medium overhang rudder vl6Rl6, the overhang balance tending to have somewhat lower hinge moments at the high rudder deflections.

Sealing the various overhangs had, in general, very little effect on the value $C_{h\delta_r}$, but sealing the hinge of the internally

balanced rudder reduced the negative value of Ch from -0.0045

to -0.0035.

Results of the 50 percent overhang rudder indicate a greater tendency for rudder force reversal at high rudder deflections and high angles of attack of opposite sign than for the rudders with smaller overhang balances, since the hinge-moment curves show greater tendency for over balance. This effect is much more marked for the case with the unsealed rudder gap.

Tab characteristics. Tab tests on the plain rudder (figs. 9 to 12 and 22 to 25) indicate that for angles of attack of zero to stall, and rudder angles ±30°, the tab is effective to about ±20°. The results indicate that a tab deflection of about 10° will trim out about 6° of rudder deflection, and that the tab effectiveness, clet is about 0.005 or about one-sixth as effective as the rudder.

The tab hinge-moments results (fig.23) indicate almost linear hinge-moment characteristics for tab deflections at least as great as ±20°, the largest deflections tested. The variation of tab hinge moment with rudder deflection is given in figure 24. Sealing the tab gap had little effect on the tab hinge moment up to rudder deflections of about 15° (fig. 25). The effect of rudder-balance configuration on the tab hinge moments can be seen for zero tab and zero angle of attack on figure 25. They show little effect of balance configuration for rudder angles of ±15.

Effect of transition. The transition was fixed near the leading edge of the vertical tail and stub fuselage by means of a 0.013-inch-diameter wire placed at the 10-percent-chord station along the vertical surface of the plain rudder, $V^{14}R^{14}$, and around the stub fuselage back of the leading edge. In order to be able to obtain direct comparison of the data for free transition and fixed transition, some of the data of figures 6 and 13 have been replotted in figure 26. Fixing transition shifted all of the curves slightly and reduced the value of $C_{h\delta r}$ (table II)

over the small rudder-deflection range and, in general, reduced the hinge moments over most of the angle of attack and rudderdeflection range.

CONCLUSIONS

The data presented indicate the following conclusions:

- 1. The internally balanced and overhang balanced rudders that have about the same balance area have about the same hingement characteristics throughout the angle-of-yaw and rudder-angle range.
 - 2. Sealing the nose of the overhang balance increased the rudder effectiveness in producing lift, the greater increase being obtained for intermediate balance size.
 - 3. Completely sealing the balance of the internally balanced rudder resulted in lower hinge moments and higher lift effectiveness than were obtained with the hinges unsealed.

4. The results of the tab tests indicated that the tab was effective at least to tab angles of ±20° over the rudder-deflection range, except for the case of large positive angles of attack combined with large negative rudder deflections.

Langley Memorial Aeronautical Laboratory
National Advisory Committee for Aeronautics
Langley Field, Va.

REFERENCE

1. Sears, Richard I.: Wind-Tunnel Data on the Aerodynamic Characteristics of Airplane Control Surfaces. NACA ACR No. 3L08, 1943.

TABLE I

GEOMETRIC CHARACTERISTICS OF THE 0.45-SCALE

MODEL OF THE XP-62 VERTICAL

TAIL

Vertical tail, sq ft	0.26
Vertical tail height, ft	4.97
Vertical tail aspect ratio	2.40
Rudder area (aft of hinge line) sq ft	+.28
Rudder balance area, sq ft	
V ¹⁴ R ¹⁴ Mini	lmum
V16 R16	.855
V16 R16.5	
V ¹⁸ R ¹⁸ 1.	
Horizontal tail area, sq ft	7.7

TABLE II

Tail surface	Rudder gap	C _L a	CLSr	Char	C _{hor}
VI4 RI4	Unsealed Sealed	0.050	0.030	0.0010	-0.0051 0050
Horizontal tail off	Unsealed	.048	.028	.0011	0060
Transition fixed	Unsealed	.048	.030	.0010	0042
V16 R16	Unsealed Sealed	.047	.026	,0009	0044 0045
v16 R16.5	Hinges unsealed	.048	.032	.0012	0045
	Hinges sealed	.048	.035	.0012	0035
v18 R18	Unsealed Sealed	.049	.028 .032	.0023 .0025	0020 0020

and the same of the same the first of the contract of t

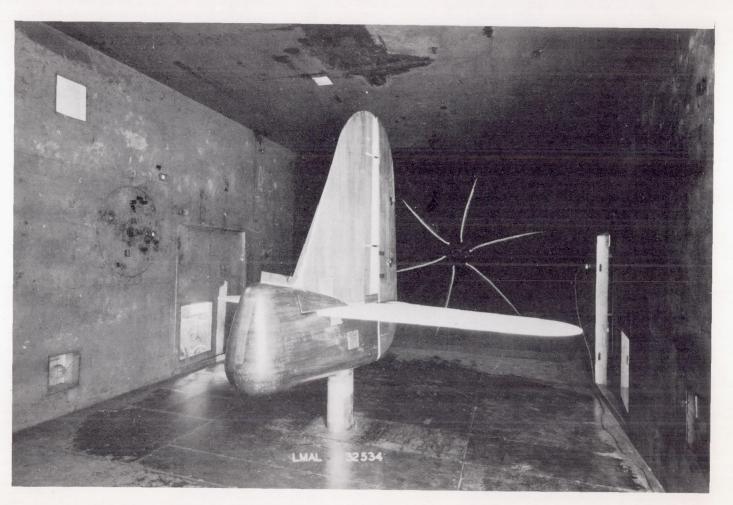
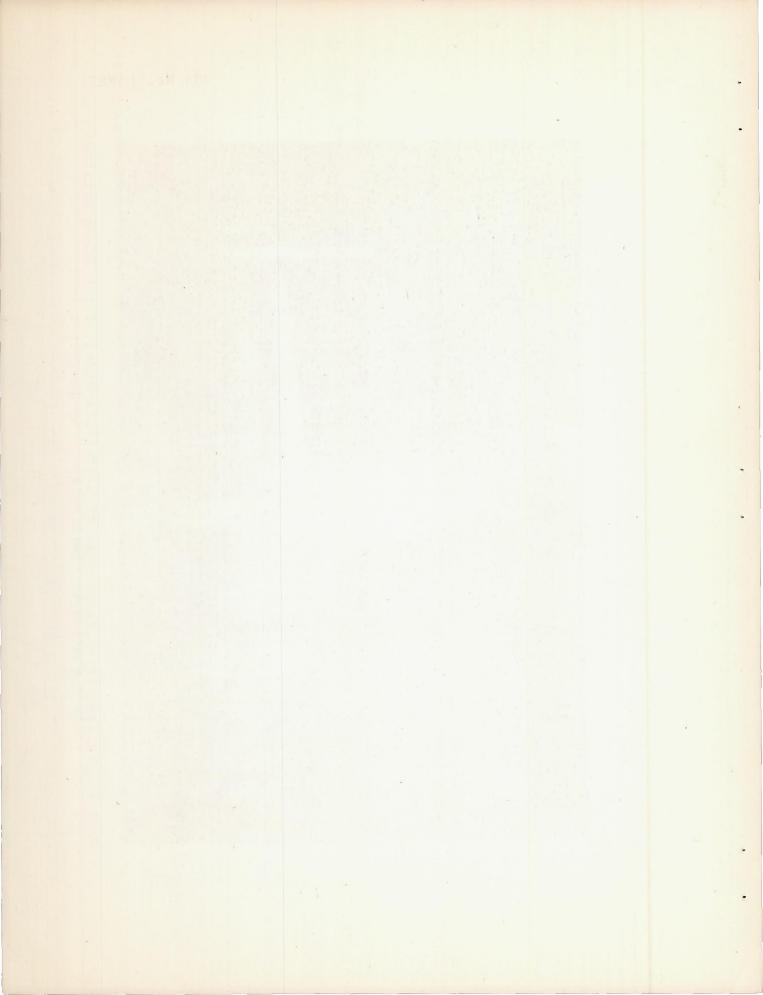


Figure 1.- Three-quarter front view of 0.45-scale model of the XP-62 vertical tail installed in the Langley 7- by 10-foot tunnel.



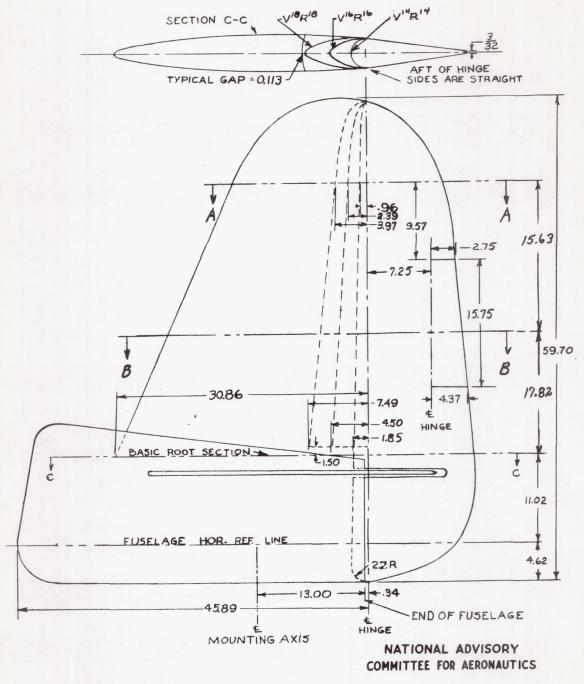
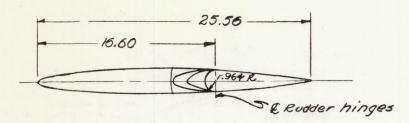


Figure 2 - Plan and section views of VIARIA, VIGRIA, and VIBRIB 0.45-scale vertical tails of XP-62 airplane.



Section A-A Leading edge radius

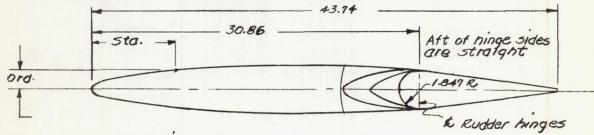
30% Balance

50% Balance

5ta 0 239478 7/7 956 1.19 143 1.671.91 2.15 2.27 2.30 2.35 240 500 - 34.51 30% Balance 23.29

16 gap 50% Balance * Rudder hinges Plain rudder Section B-B

Leading edge radius .211



Section C-C

Leading edge radius .284

30 % Balance

50% Balance

Sta 0 450,8991,351/80 225,270 3.15 360404.264.57 14.38 14.50 5.ta 0 .749 1.50 2.25 3.00 3.75 14.50 5.25 6.00 6.74 7.11 7.27 7.35 7.49 Ord 1.75 1.73 1.70 1.66 1.60 1.65 1.60 1.65 1.63 1.25 1.05 7.65 .55 14.25 .312 0

Hinge line at sta. O

NATIONAL ADVISORY COMMITTEE FOR AERONAUTICS

Figure 2 - Concluded.

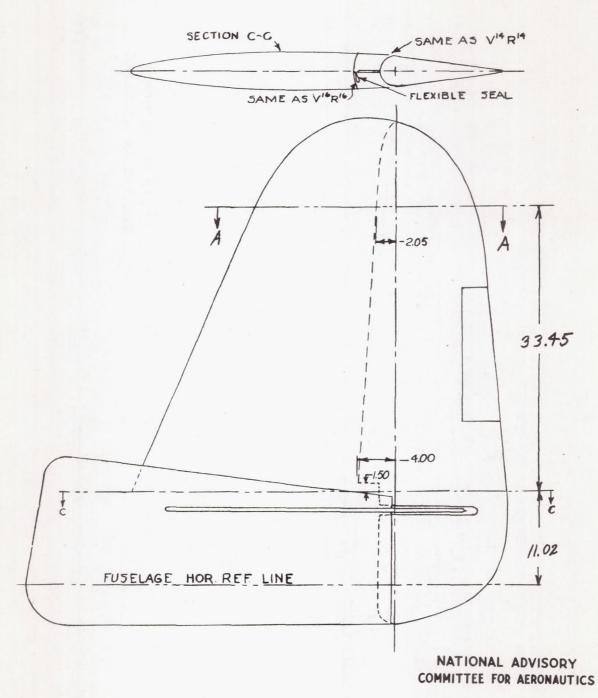
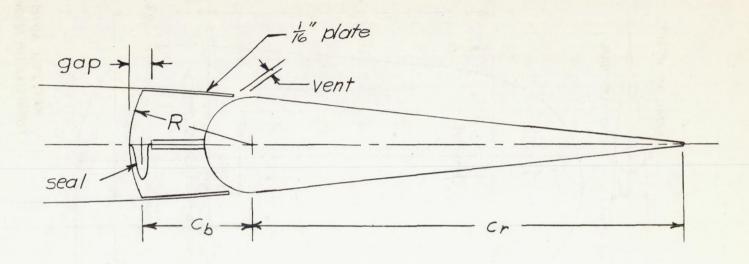


Figure 3.-Plan and section views of $V^{16}R^{16.5}$ 045-scale vertical tail of XP-62 airplane.



56	ection	cb/cr	gap/cr	vent/cr	RICT	seal /	length/cr
A	-A	.254	.051	013	.280	about	17
C	- C	.334	.047	.009	.358	about	.20

NATIONAL ADVISORY
COMMITTEE FOR AERONAUTICS

Figure 3 .- Concluded.

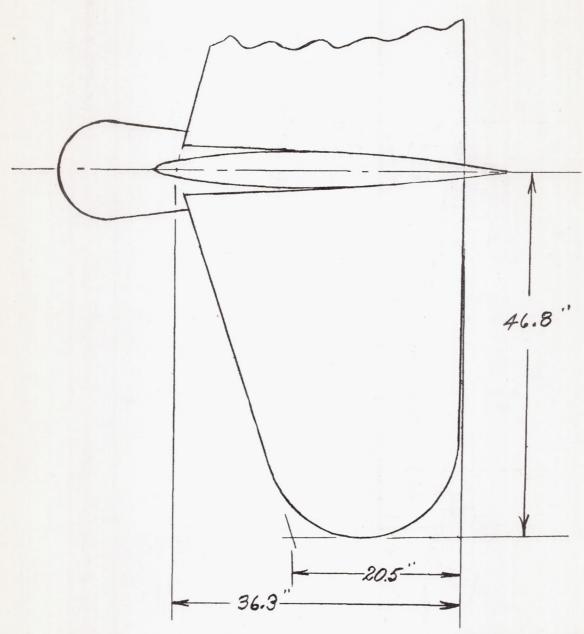
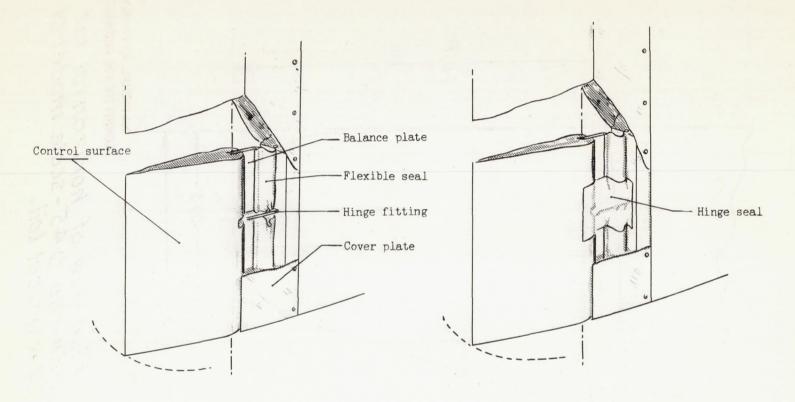


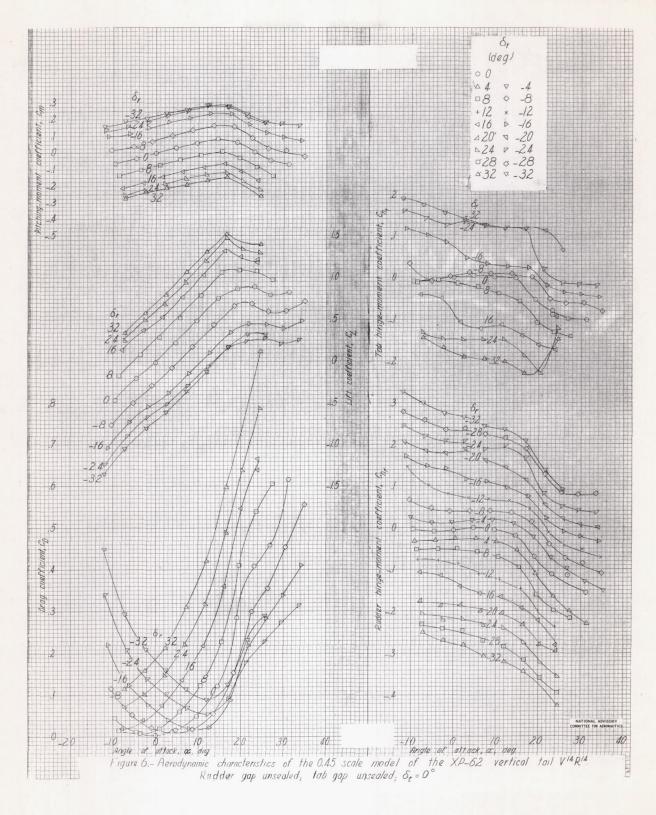
Figure 4.- Plan view of horizontal tail tested with the 0.45-scale model of the XP-62 vertical tail.

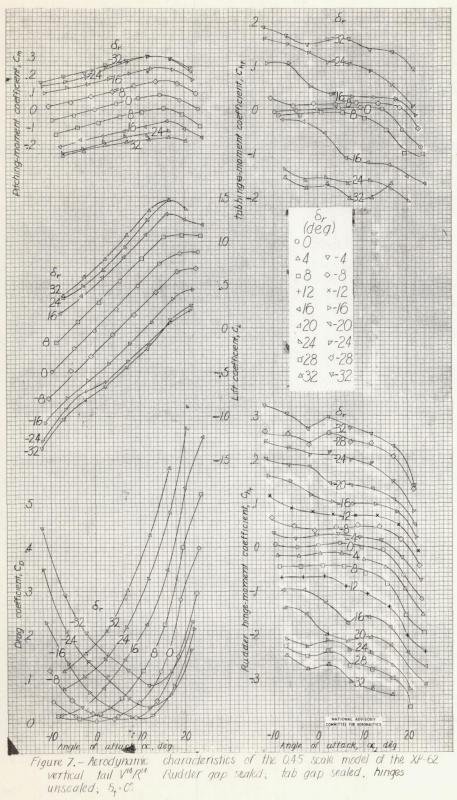


(a) Hinge not sealed.

(b) Hinge completely sealed.

Figure ${\bf 5}$. - Seal arrangement for internally balanced control surface.





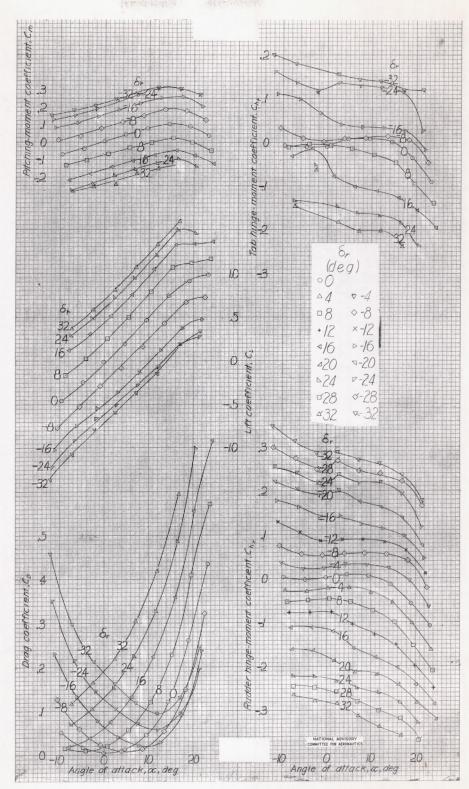


Figure 8. - Aerodynamic characteristics of the 0.45 scale model of the XP-62 vertical tail $V^{14}R^{14}$ Rudder gap unsealed; tab gap unsealed; $\delta_{\epsilon}=0$; horizontal tail off.

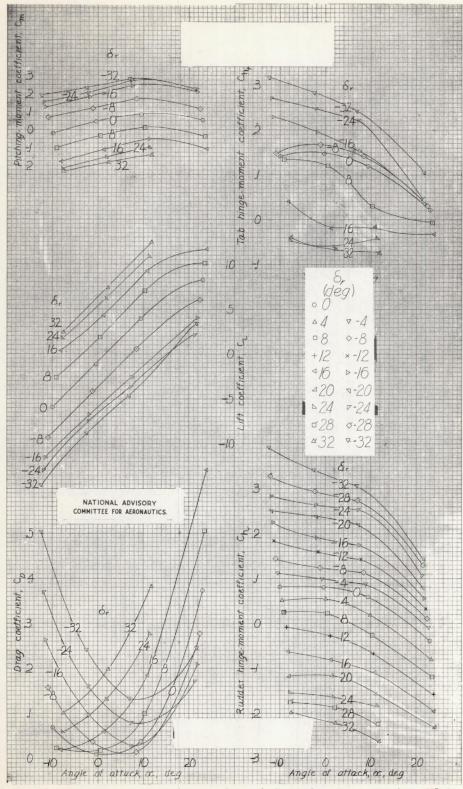


Figure 9. – Aerodynamic characteristics of the 0.45 scale model of the XP-62 vertical tail $V^{14}R^{14}$ Rudder gap unsealed; tab gap unsealed; $\delta_{\rm t}^*$ -20°.

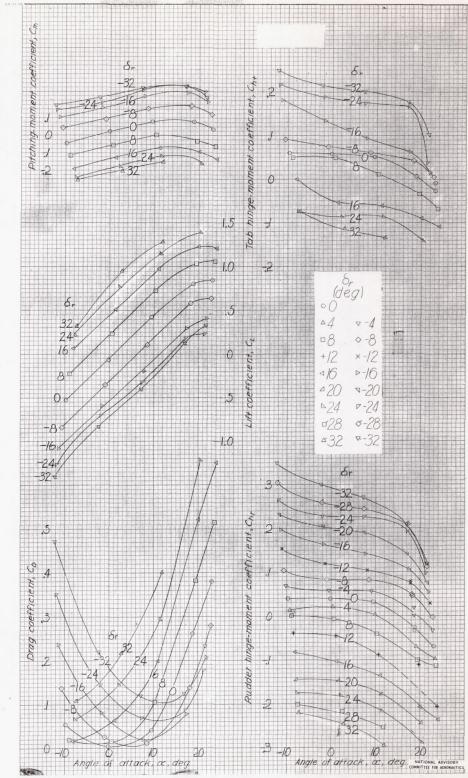


Figure 10.- Aerodynamic characteristics of the 0.45 scale model of the XP-62 vertical tail V'''R''' Rudder gap unsealed; tab gap unsealed; δ_{+} =10"

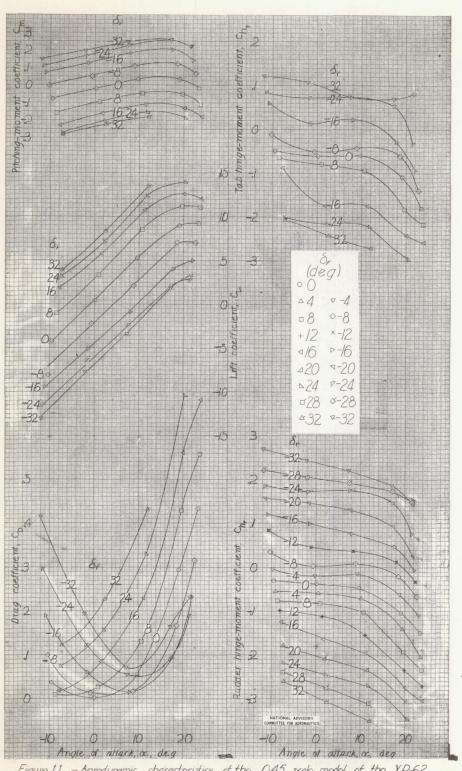


Figure 11.—Aerodynamic characteristics of the 0.45 scale model of the XP-62 vertical tail V¹⁴R¹⁴. Rudder gap unsealed, tab gap unsealed; **8**, 10°.

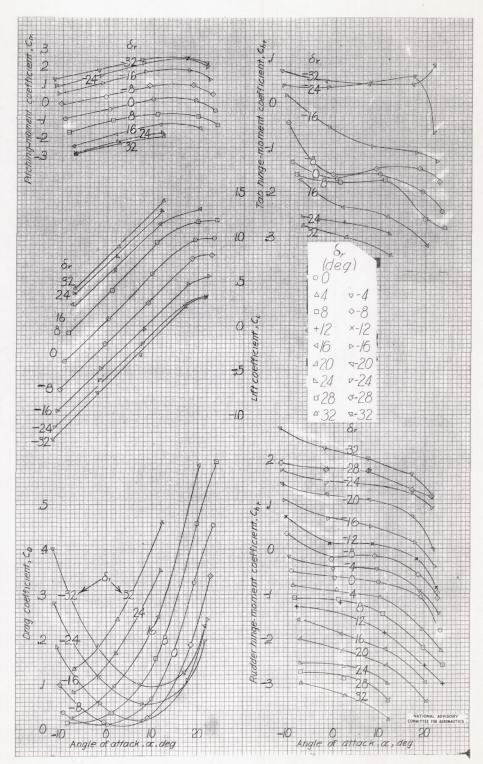


Figure 12.—Aerodynamic characteristics of the 0.45 scale model of the XP-62 vertical tail $V^{14}R^{14}$ Rudder gap unsealed; tab gap unsealed, δ_t =20°.

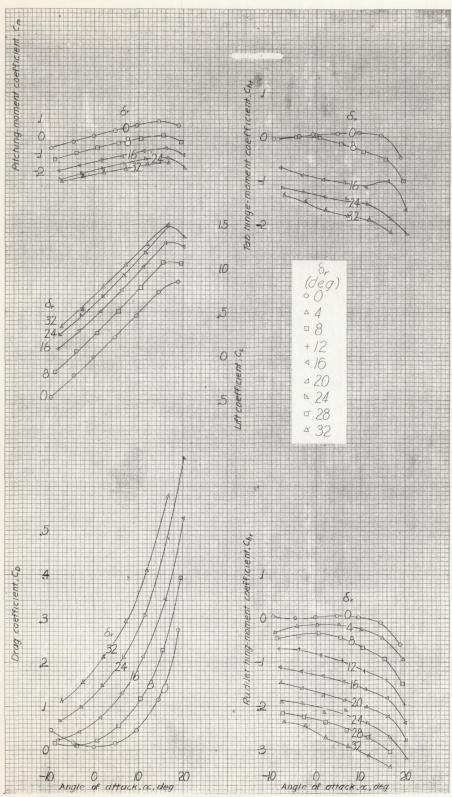


Figure 13-Aerodynamic characteristics of the 0.45 scale model of the XP-62 vertical tail V¹⁴ R¹⁴ Rudder gap unsealed; tab gap unsealed; δ_{ij} 0°; transition wire 017.

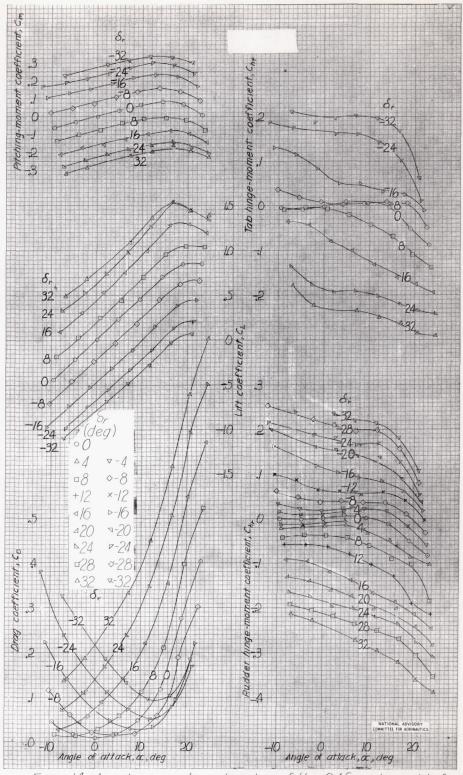


Figure 14-Aerodynamic characteristics of the 0.45 scale model of the XP-62 vertical tail V'6R'6 Rudder gap unsealed; tab gap unsealed; δ_{+} =0.

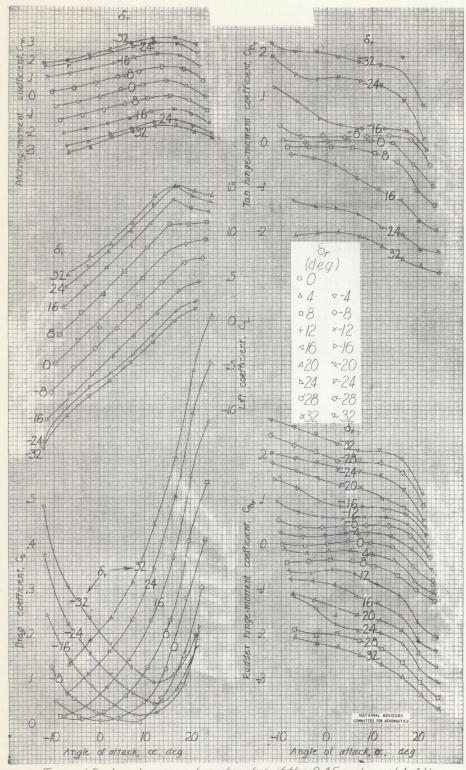


Figure 15.-Aerodynamic characteristics of the 0.45 scale model of the XP-62 vertical tail V"R" Rudder gap sealed; tab gap unsealed; hinges unsealed; 8,-0°

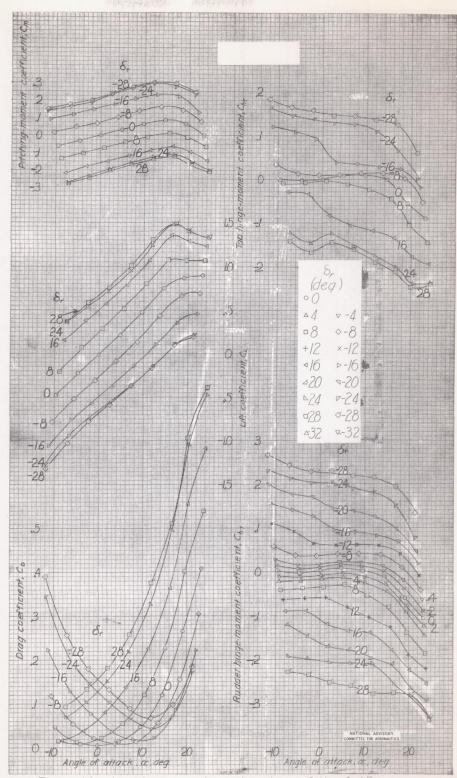


Figure 16.- Aerodynamic characteristics of the 0 45 scale model of the XP-62 vertical tail V⁶R⁶⁵ Rudder gap sealed, tab gap unsealed, hinges unsealed, S; 0°

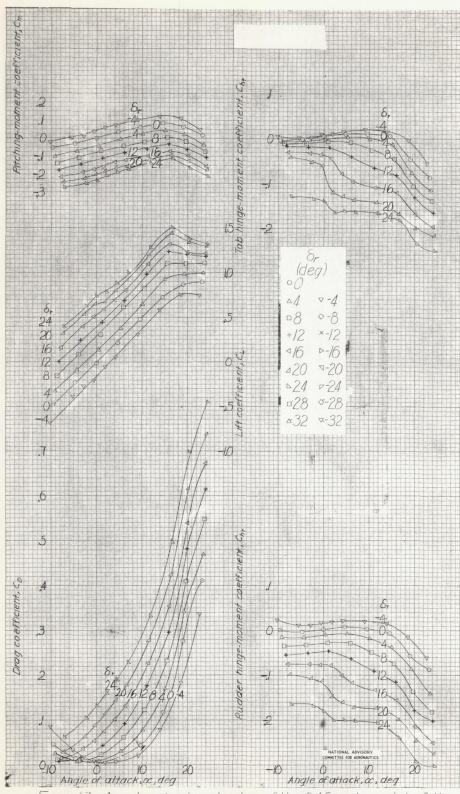


Figure 17. - Aerodynamic characteristics of the 0.45 scale model of the XP-6.2 vertical tail $V^{*}R^{**s}R$ udder gap sealed; tab gap unsealed, hinges sealed; $\delta_{F}=0$

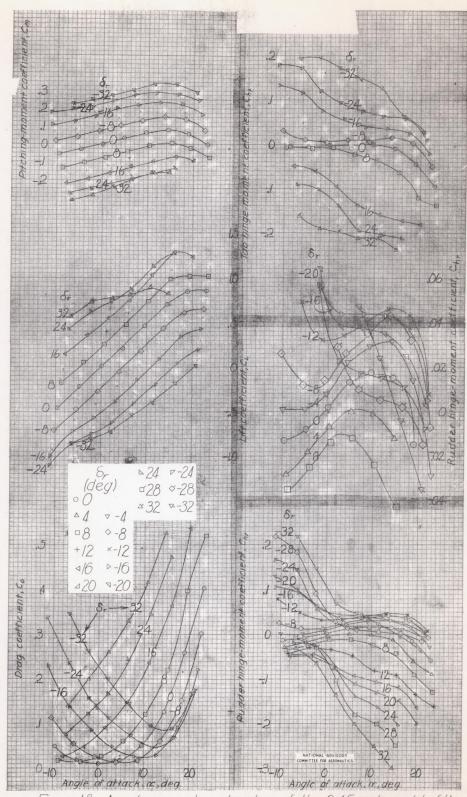


Figure 18.- Aerody namic characteristics of the 0.45 scale model of the XP-62 vertical tail V°R°. Rudder gap unsealed; tab gap unsealed; \$,=0.

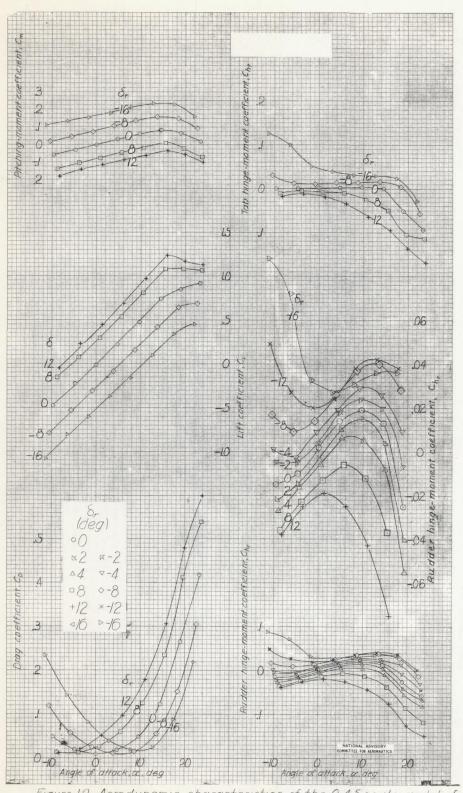
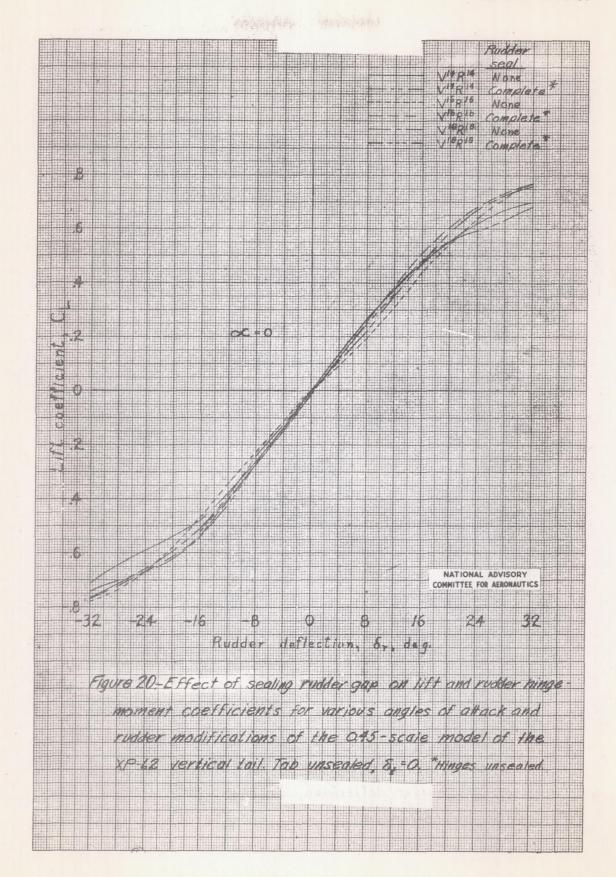
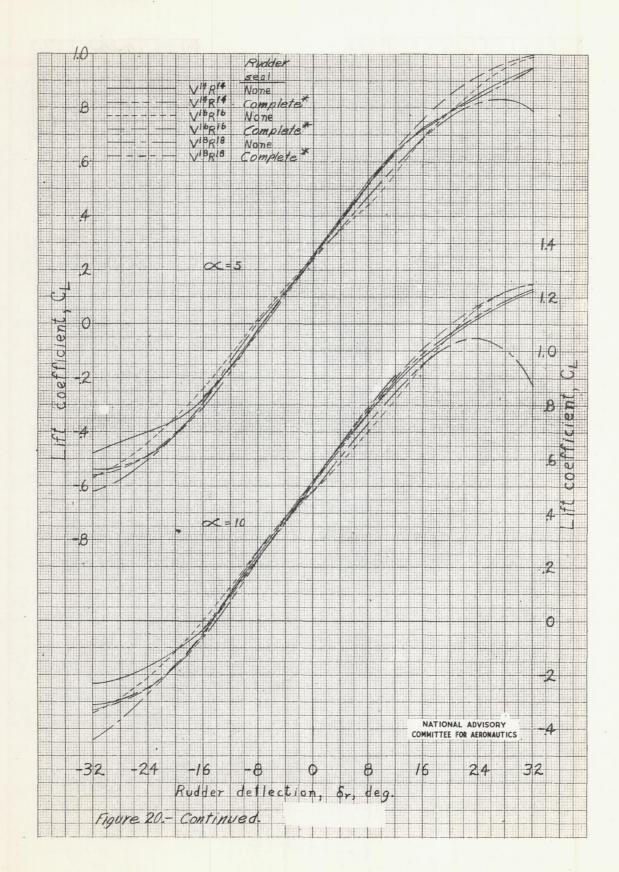
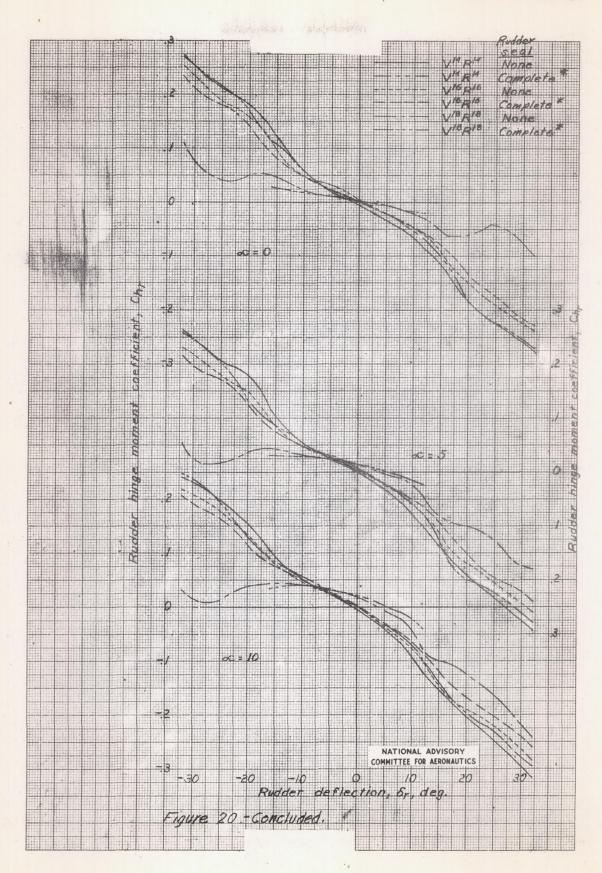


Figure 19.-Aerodynamic characteristics of the 0.45 scale model of the XP-62 vertical tail V"R" Rudder gap sealed; tab gap unsealed; hinges unsealed; 8,=0°







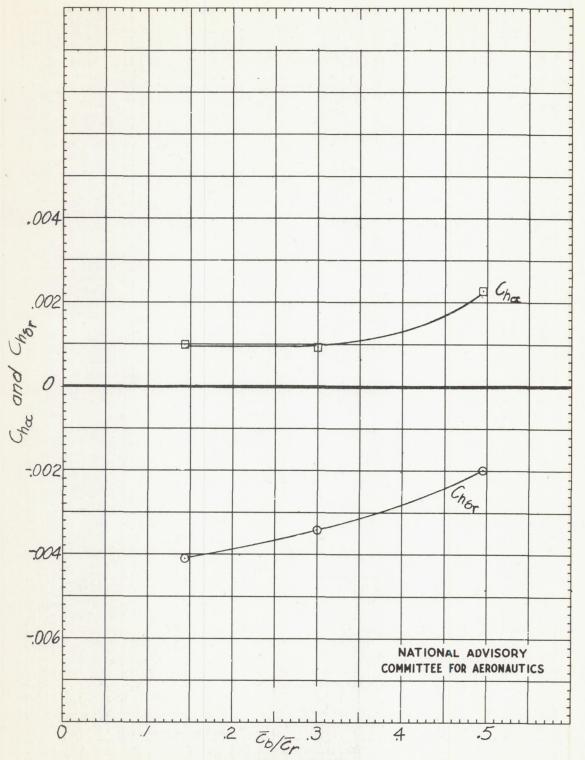
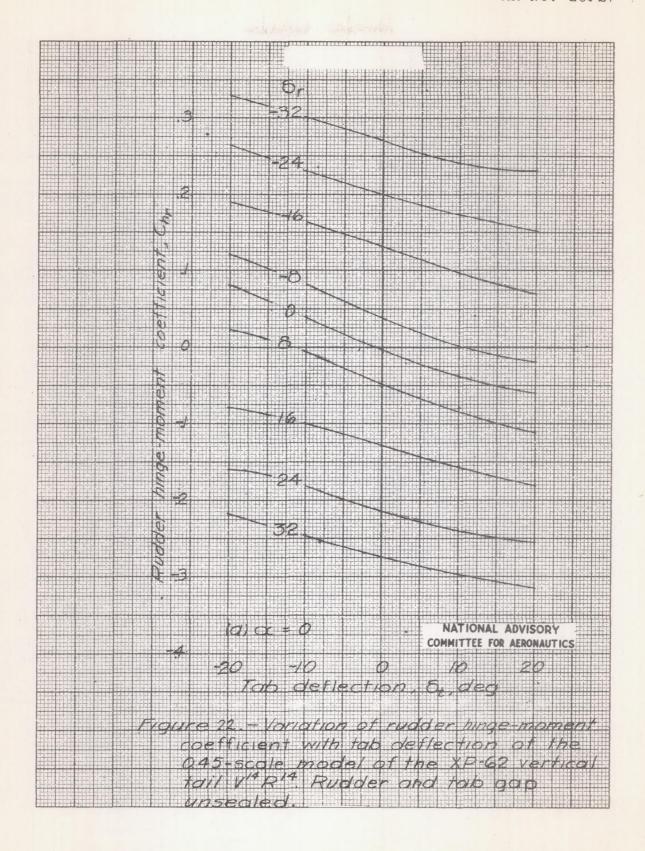
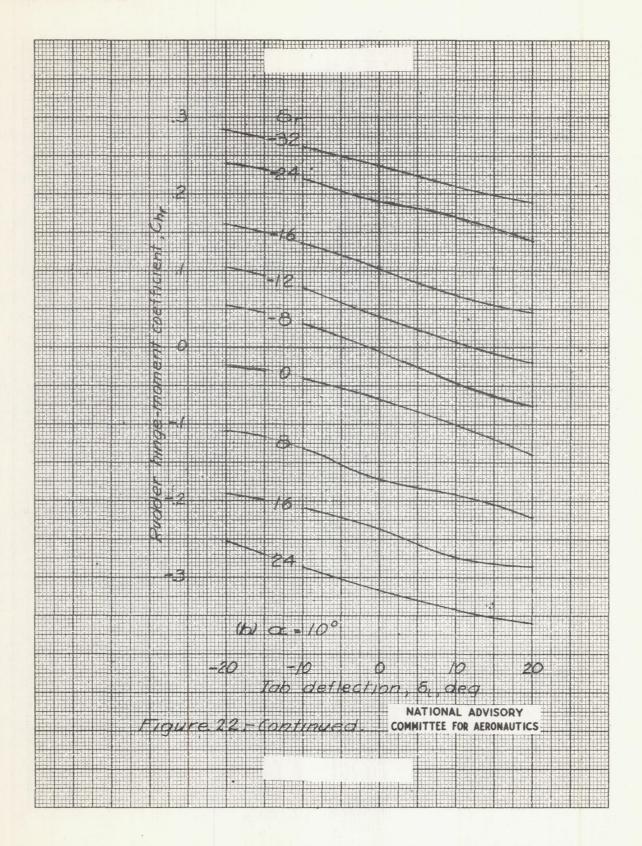
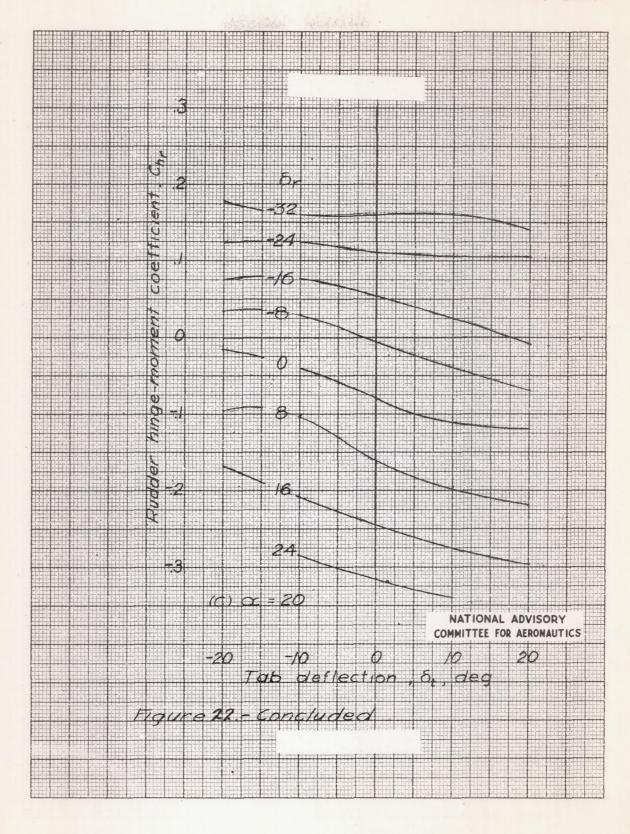
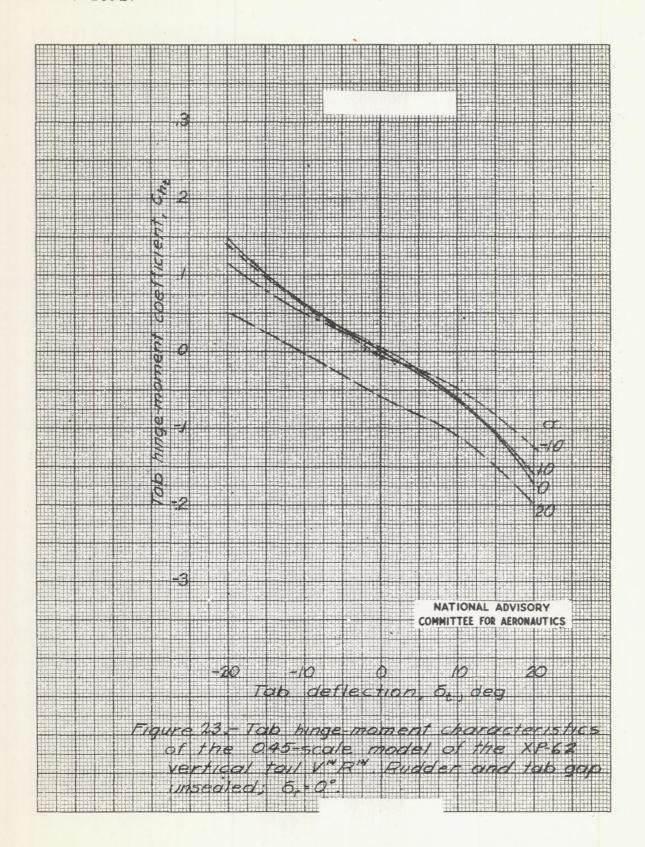


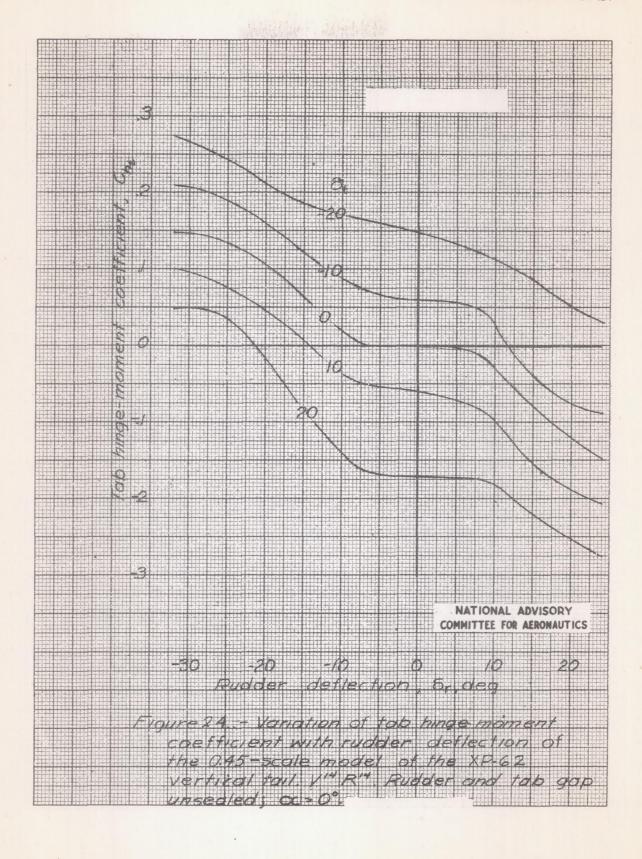
Figure 21.-Variation of the parameters C_{ha} and C_{har} with the ratio C_b/C_r for the 0.45-scale model of the XP-62 vertical tail Rudder gap and tab gap unsealed.

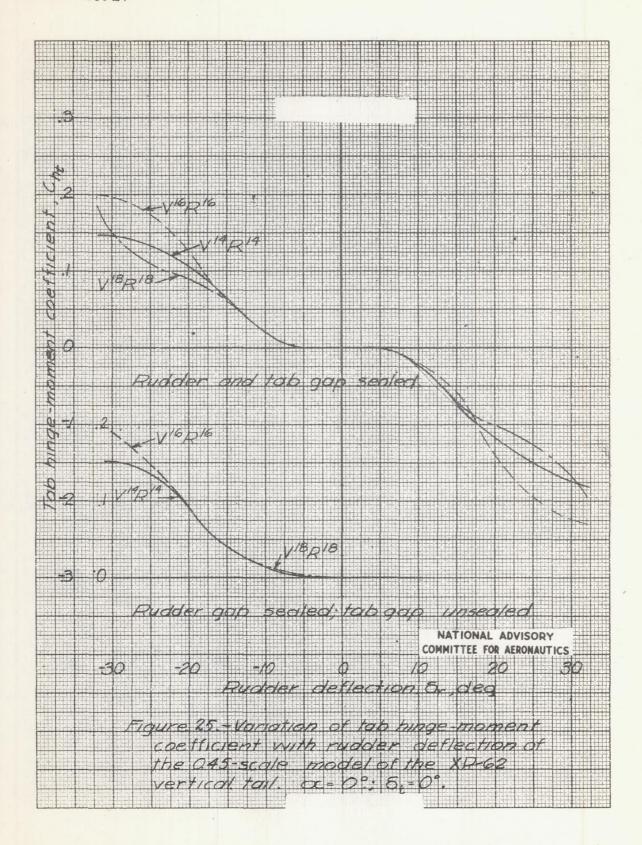


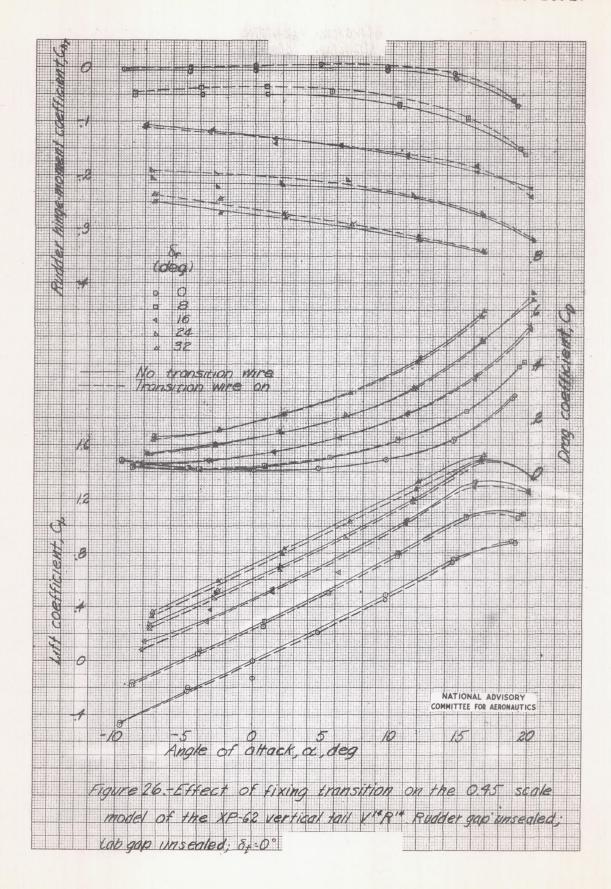












- REPRODUCTION SERVICE CONTRACTOR

